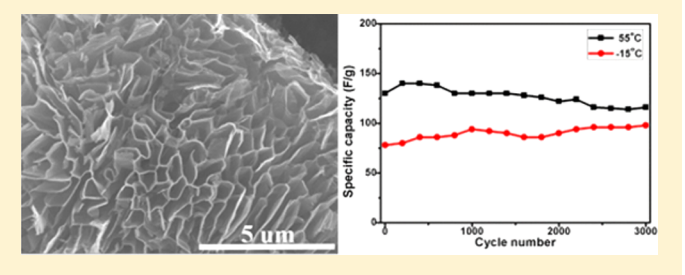
✓ Cite This: Ind. Eng. Chem. Res. 2018, 57, 3610-3616

Design and Synthesis of 3D Potassium-Ion Pre-Intercalated Graphene for Supercapacitors

Liang Chang, Dario J. Stacchiola, and Yun Hang Hu*, So

Supporting Information

ABSTRACT: In this paper, a novel material—3D potassiumion preintercalated graphene—was designed and synthesized via one step using a new reaction between K and CO. Furthermore, this material exhibited excellent performance as electrodes for aqueous symmetrical supercapacitors. When the electrode was scaled up from 3.0 to 8.0 mg/cm², negligible capacitance degradation was observed, leading to a very high areal capacitance of 1.50 F/cm² at 1 A/g. Furthermore, even if a large operating temperature of −15 or 55 °C was employed,



its excellent electrochemical performance remained with specific capacitances of 208 F/g at 55 $^{\circ}$ C, 184 F/g at 25 $^{\circ}$ C, and 98 F/g at -15 $^{\circ}$ C. This could be attributed to 3D structure and K⁺ preintercalation of the material, which provides rich active sites for electric double-layer formation, lower ion transport resistance, and shorter diffusion distance.

1. INTRODUCTION

The rising concern of environmental issues has pushed forward utilization of clean energies and development of their storage devices. 1,2 Supercapacitors as electrical storage devices have been widely applied in portable consumer electronics, electric vehicles, and large-scale grid due to their high power density, long cycle life, excellent reversibility, and wide operating temperature range.^{3,4} One type of supercapacitors is electric double-layer capacitors, in which charge storage is achieved by forming electric double layers at the interface of electrolyte and electrode. This potential-derived surface charge storage mechanism ensures their fast charge transfer kinetics and reversible electrostatic adsorption/desorption, leading to highrate performance and excellent reversibility. 5,6 Ideal electrode materials for double-layer capacitors should have large accessible surface areas and continuous charge transfer pathways. It is well-known that high gravimetric and volumetric capacitances are usually achieved by decreasing mass loading of electrodes for short diffusion distance. However, this approach is not practical because a high mass loading of electrodes is required to reach a large cell capacitance for a commercial supercapacitor. Furthermore, a wide operating temperature range is important for a supercapacitor to provide stable energy storage in a harsh environment. \$\frac{1}{8}-10\$ Therefore, an efficient supercapacitor would possess high electrochemical performance with a large mass loading of electrodes under a wide operating temperature range.

Graphene, as a promising electrode material for supercapacitors, can be modified by (1) KOH activation to improve the ratio of mesopores and macropores, 11,12 (2) threedimensional structure to increase accessible surface area and improve charge transfer kinetics, ^{13–15} and (3) functional group formation to introduce pseudocapacitance. 16 Furthermore, electrolyte-ion preintercalation into electrode materials has been demonstrated as an effective method to further enhance electrochemical performance. Yang et al. constructed electrolyte-mediated chemically converted graphene (EM-CCG) films by a capillary compression procedure. The EM-CCG films can achieve a high volumetric capacitance of 200 F/cm³ and high volumetric energy density of 59.9 Wh/L with mass loading of 10 mg/cm². Mai et al. 18 lithiated MoO₃ nanobelts with a LiCl as the lithium source by an ultrasonic/stirring-assistant hydrothermal method, which can receive enhanced Li storage capability. These capacitance improvements by electrolyte-ion preintercalation were attributed to lowering ion transfer resistance, stabilizing electrode materials and providing more effective active sites for electrostatic adsorption. 17,18 However, those electrolyte ions preintercalation processes consumed more time and energy. To solve the issue, in this work, we designed a simplified approach, in which a one-step reaction between K and CO can not only construct 3D graphene but also preintercalate K⁺ into the graphene matrix. The aqueous symmetrical supercapacitor with the novel material as electrodes can reach areal capacitance of 1.50 F/cm² and a wide operating temperature range of -15 to 55 °C.

Received: January 3, 2018
Revised: February 10, 2018
Accepted: February 22, 2018
Published: February 22, 2018

[†]Department of Materials Science and Engineering, Michigan Technological University, 1400 Townsend Drive, Houghton, Michigan 49931-1295, United States

[‡]Center for Functional Nanomaterials, Brookhaven National Laboratory, Upton, New York 11973, United States

[§]School of Environmental Science and Engineering, Shanghai Jiao Tong University, Shanghai 200240, China

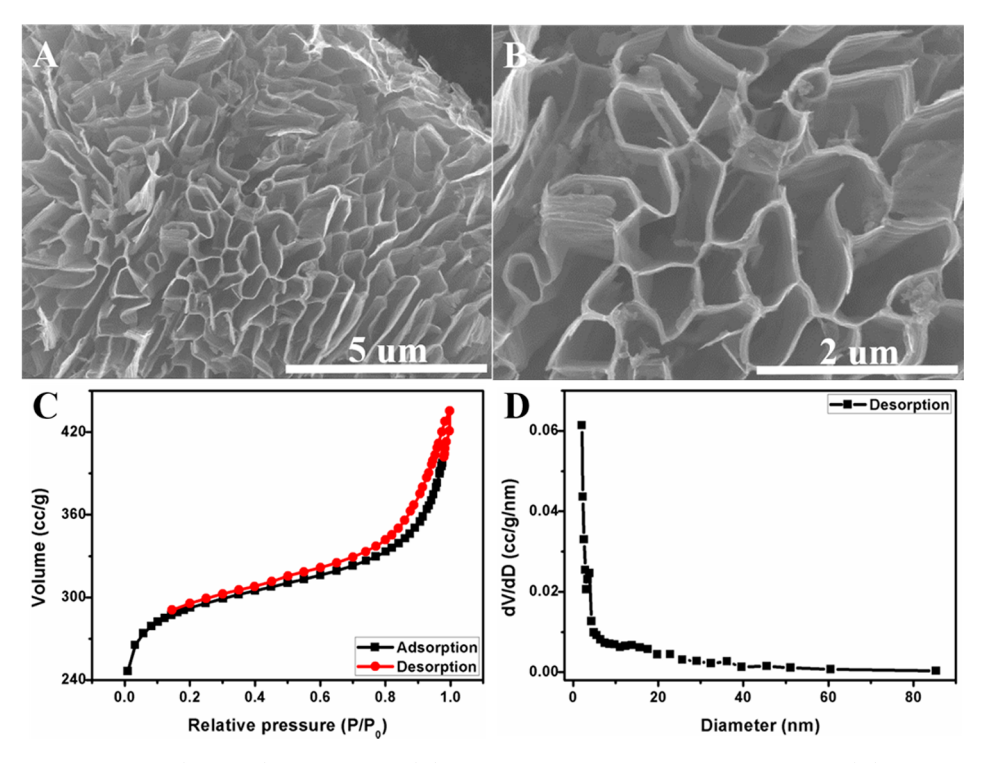


Figure 1. 3D KIPIG characterization: (A and B) SEM images, (C) N2 adsorption and desorption curves, and (D) its pore size distribution.

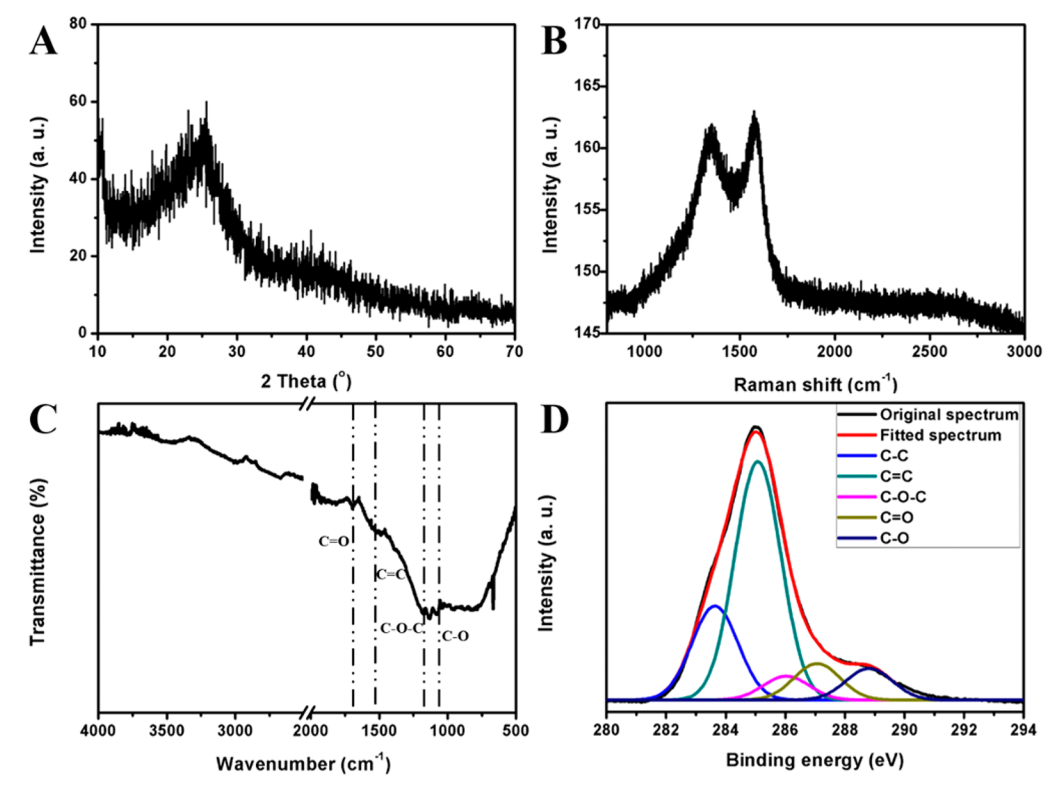


Figure 2. (A) XRD pattern, (B) Raman spectrum, (C) FTIR pattern, and (D) XPS spectra at C 1s of 3D KIPIG.

2. RESULTS AND DISCUSSION

To synthesize 3D graphene with preintercalated electrolyte ions, we designed the reaction between liquid potassium and CO gas as follows:

$$2K(1) + 3CO(g) = 2C(graphene)(s) + K2CO3(s)$$
 (1)

It is a thermodynamically favorable reaction due to negative enthalpy change (-811.643 kJ/mol) and Gibbs free energy change (-369.784 kJ/mol). Furthermore, its feasibility was demonstrated by reacting K with 50 psi CO at 500 °C. First, in this process, potassium ion, which is a commonly used electrolyte ion for aqueous supercapacitors, has been successfully preintercalated into graphene matrix; namely,

Industrial & Engineering Chemistry Research

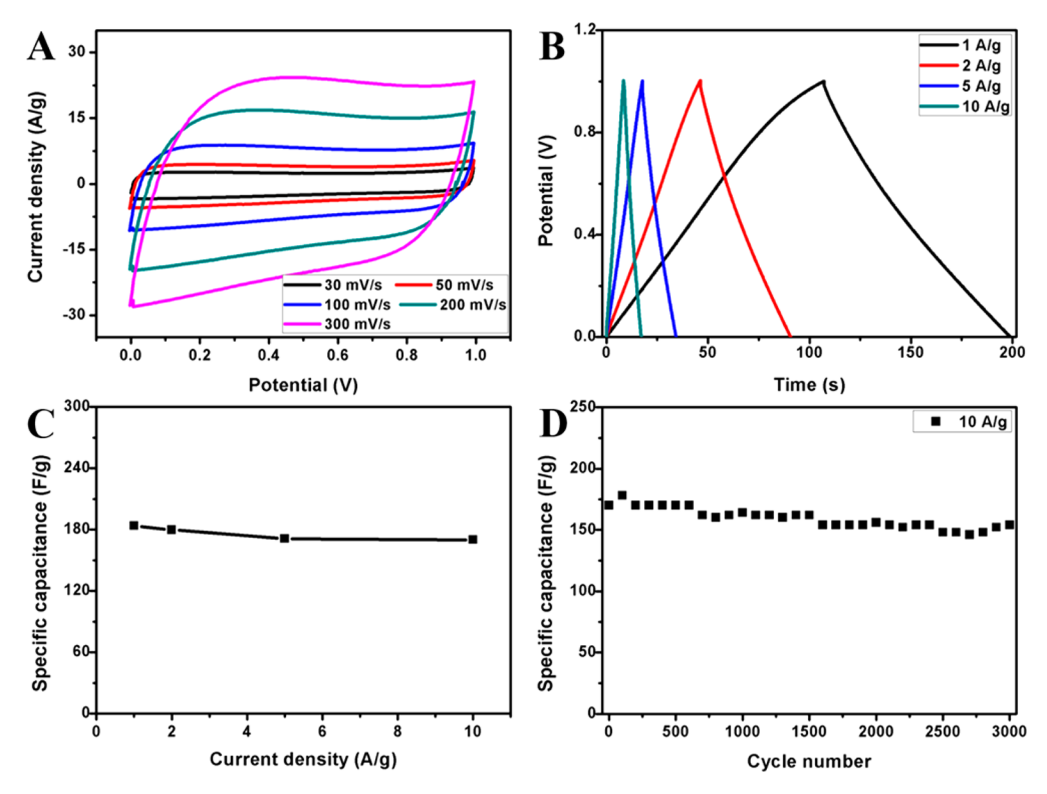


Figure 3. Electrochemical performance of 3D KIPIG electrodes with mass loading of 3 mg/cm²: (A) CV curves at scan rates of 30-300 mV/s, (B) galvanostatic charge/discharge profiles at current densities of 1-10 A/g, (C) current densities vs specific capacitances, and (D) cycling stability test for 3000 cycles at current density of 10 A/g.

ICP and EDS measurements showed 0.23 and 0.24 wt % K+ intercalated in the graphene, respectively. The simultaneously formed K2CO3 from the reaction between K and CO can isolate graphene sheets to avoid graphite formation and control graphene shape. As shown in Figure 1A,B, graphene sheets were bent and coiled, leading to three-dimensional flowerstructured graphene. The layer structure of the 3D graphene was confirmed by TEM image (Figure S3). The 3D K+preintercalated graphene was conducted with the N2 adsorption/desorption test at 77 K. N₂ adsorption/desorption curves show type II isotherm with a H3 hysteresis loop (Figure 1C), indicating porous structure. Its surface area calculated from the N_2 adsorption with BET model is 990 m²/g. The pore sizes are concentrated in the range of 5-20 nm (Figure 1D), demonstrating the existence of mesopores and macropores. Xray diffraction (XRD) was also employed to characterize the structure of the graphene. As shown in Figure 2A, one can see two peaks at 25.5° and 43°, which belong to (002) and (101) planes, respectively. 19 The thickness of the graphene, which was calculated from the XRD peaks, is three layers. Its defect structure was demonstrated by Raman spectrum. Figure 2B shows the D-band at 1350 cm⁻¹ (sp³ carbon atoms associated with functional groups) and G-bands at 1580 cm⁻¹ (sp² carbon atoms associated with graphene sheets). The functional groups were further evaluated by Fourier transform infrared (FTIR) spectrum (Figure 2C). IR bands at 1066 cm⁻¹, 1250 cm⁻¹, and 1725 cm⁻¹ can be attributed to C-O, C-O-C, and C=O vibrations, respectively. C=C stretching vibration can also be observed at 1576 cm⁻¹. Those were supported by X-ray photoelectron spectroscopy (XPS) measurements. As shown in Figure 2D, the C 1s XPS curve was deconvoluated into 5 peaks, in which peaks at 286, 287.3, and 288.5 eV can be attributed to C-O-C, C=O, and C-O groups, respectively. The additional

peaks at 283.7 and 285.0 eV can be assigned to C-C and C=C groups, respectively. Furthermore, oxygen content was determined by element analysis (12.12 wt %) and EDS test (13.46%). Therefore, one can conclude that the synthesized graphene possesses 3D structure with the intercalated K ions and the oxygen functional groups as well as meso-/macropores, constituting its unique properties as electrode materials for supercapacitors. The K ion preintercalated graphene is denoted as KIPIG.

A symmetrical aqueous supercapacitor with two identical KIPIG electrodes, a separator, and 2 M KOH electrolyte was assembled to test the electrochemical performance of KIPIG material. Cyclic voltammetry conducted at potential range from 0 to 1 V shows good electric double-layer performance at scan rate of 30 mV/s with a rectangular CV curve (Figure 3A). Even at higher scan rates up to 300 mV/s, one can see larger CV areas with negligible polarization, indicating more charge propagation on the KIPIG surface without obviously increased resistance. 20,21 Those results were supported by galvanstatic charge/discharge profiles with symmetrical triangle lines (Figure 3B). The specific capacitance of KIPIG electrodes achieves 184 F/g at current density of 1 A/g and 170 F/g even when current density was increased 10 times. As shown in Figure 3C, one can see excellent rate performance with a capacitance retention of 92.4%. Furthermore, KIPIG electrodes possess excellent reversibility; namely, after 3000 galvanostatic charge/discharge cycles at current density of 10 A/g, the specific capacitance can be still 154 F/g with a 90.6% capacitance retention (Figure 3D). The excellent electrochemical performance can be attributed to unique properties of KIPIG: The high capacitance and good rate performance are due to 3D structure and meso-/macroporous structure, which can effectively prevent graphene aggregation and provide

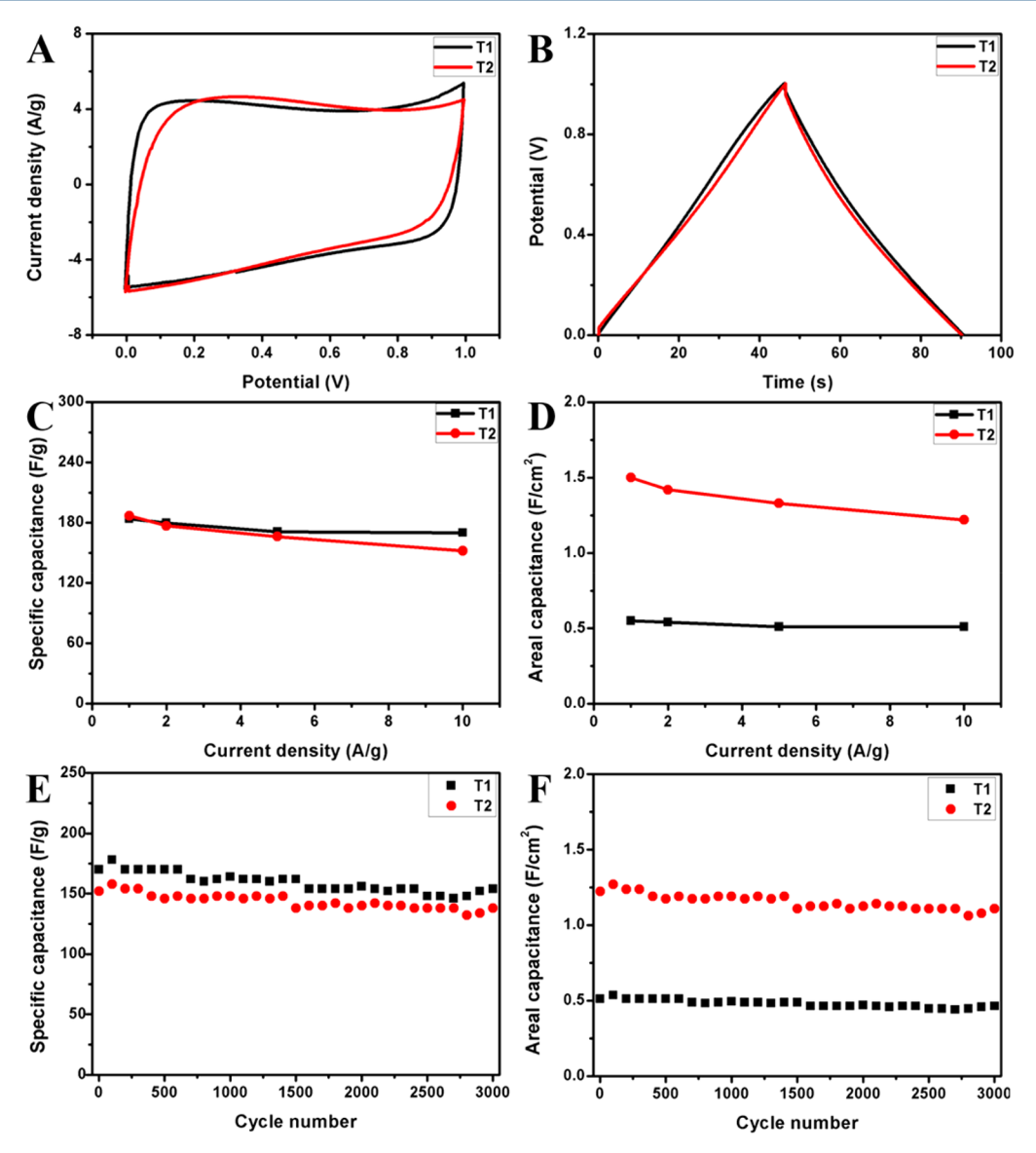


Figure 4. Mass loading influence on electrochemical performance of 3D KIPIG electrodes (T1:3 mg/cm²; T2:8 mg/cm²): (A) CV curves at scan rate of 30 mV/s, (B) galvanostatic charge/discharge profiles at current density of 2 A/g, gravimetric capacitances (C) and areal capacitances (D) at different current densities, stability test for gravimetric capacitance (E), and areal capacitance (F).

continuous ion transport route and large electrolyte-ion-accessible surface area. 22,23 The excellent cycling performance might be associated with the stable structure of KIPIG, which is reflected by the observation that even after 3000 galvanostatic charge/discharge cycles, the 3D flower-like structure of KIPIG still remained (Figure S4). Besides, introducing functional groups can bring up to 15% additional capacitance and improve wettability. 24 In addition, electrolyte ion (K⁺) preintercalation can benefit electric double layer performance, especially at high current density and high mass loading via improving ion and electron transport rate. 22

To evaluate the effect of mass loading on electrochemical performance, mass loading of KIPIG electrodes was increased from 3.0 mg/cm² (T1) to 8.0 mg/cm² (T2). As shown in Figure 4A,B, the increase of mass loading resulted in negligible influence on the capacitance, which was reflected by the similar CV areas for two different mass loadings at a scan rate of 50 mV/s and discharge time at current density of 2 A/g. Furthermore, even at high mass loading (T2), KIPIG electrodes

exhibited excellent rate performance with specific capacitance of 187 F/g at 1 A/g and 152 F/g at 10 A/g (Figure 4C). Obviously, the increasing mass loading without sacrificing gravimetric capacitance can benefit areal capacitance. As a result, KIPIG electrodes exhibited a very high areal capacitance up to $1.50~\text{F/cm}^2$ for T2 (Figure 4D), which is larger than most works. The excellent cycling stability of the electrodes were obtained for high mass loading (Figure 4E,F); namely, the capacitance retention is as high as 90.7% even after 3000 charge/discharge cycles.

Finally, supercapacitors with KIPIG electrodes were examined for a wide operating temperature range. At 55 °C, rectangular CV curve without polarization at 100 mV/s (Figure 5A) and triangle galvanostatic charge/discharge line without IR drop (Figure 5B) at 1 A/g demonstrate excellent charge accumulation of KIPIG electrodes. The excellent electric double-layer performance can also be reflected by good rate capability with specific capacitance of 208 F/g at 1 A/g and 170 F/g at 10 A/g. The cycling stability at 55 °C is slightly lower

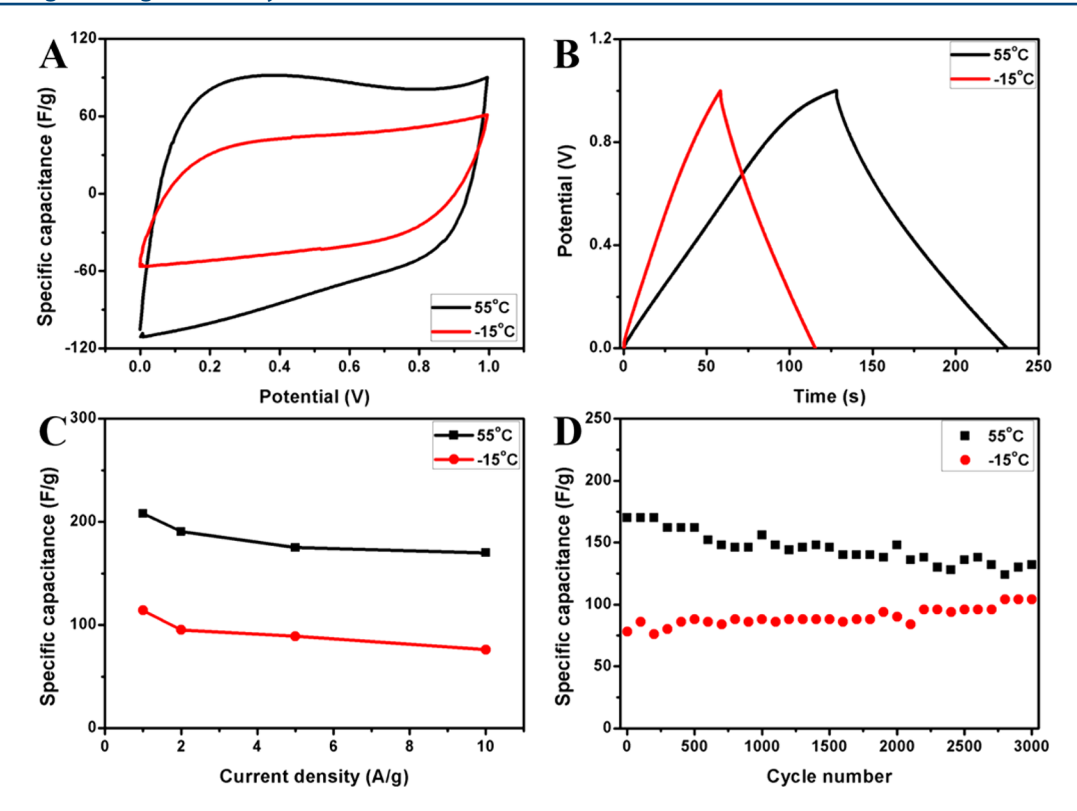


Figure 5. Electrochemical performance of 3D-KIPIG-based symmetrical supercapacitors in a wide temperature range (black line: 55 $^{\circ}$ C, red line: -15 $^{\circ}$ C): (A) CV curves at scan rate of 100 mV/s, (B) charge/discharge profile at current densities 1 A/g, (C) specific capacitances vs current densities, and (D) cycling performance at current density of 10 A/g.

than that at room temperature due to strengthened corrosion of KOH solution and lowered stability of electrode materials at high temperature condition. 25,26 Compared to those at 55 °C, both CV area and discharge time obviously decreased at -15 °C. This happened because the kinetics of ion adsorption/ desorption can be significantly reduced and charge transport rate decreased by lowering temperature.8 At 1 A/g, the specific capacitance can be 114.2 F/g at -15 °C. A huge electrolyte concentration gradient near the electrode surface further enhances capacitance degradation under the rapid charge/ discharge process (Figure 5C).²⁷ In this situation, cycling stability can reach 133.3% after 3000 cycles. It may attribute to the activation effects of produced heating during cycles.²⁸ Therefore, KIPIG electrodes can achieve ultrahigh areal capacitance in a wide operating temperature range, which makes the electrode material great potential for commercial application.

3. CONCLUSION

3D K-ion preintercalated graphene (KIPIG) can be synthesized by reacting K liquid with CO gas in one step. Furthermore, the material was successfully exploited for aqueous supercapacitors, leading to a very high areal capacitance of 1.50 F/cm², excellent rate performance up to 10 A/g, and high reversibility of 3000 cycles at 10 A/g. The specific capacitance can be 184 F/g at 1 A/g at room temperature, which is between that of 208 F/g at 55 °C and that of 114.2 F/g at -15 °C. Under the extended operating temperature from -15 to 55 °C, the excellent recycling stability was obtained, which ensured KIPIG electrodes being applied for supercapacitors even under harsh environment.

4. EXPERIMENTAL SECTION

3D K-ion preintercalated graphene (KIPIG) was synthesized by a one-step reaction between potassium liquid and CO gas. In this process, potassium ($3 \times 3 \text{ cm}^2$ block dipped in coal oil) was cut into $0.5 \times 1 \text{ cm}^2$ pieces and then placed in an Al_2O_3 boat, which was located in a ceramic tube batch reactor. After 50 psi CO gas was introduced into the reactor, it was heated to 500 °C and kept at that temperature for 12 h. After cooling the reactor down to room temperature, the obtained products were taken out and dipped into 36.5 wt % hydrochloric acid (HCl) overnight, washed with deionized (DI) water several times until PH = 7, and then dried in an 80 °C oven for 12 h. The collected product was donated as 3D K-ion preintercalated graphene (KIPIG).

Characterization of 3D KIPIG. The morphology of 3D KIPIG was obtained by field emission scanning electron microscope (FESEM, Hitachi-4700) with energy dispersive spectroscopy (EDS). Its surface area and pore size were determined by N2 adsorption/desorption at liquid nitrogen temperature (77 K) with an ASAP 2000 instrument. A Scintag XDS-2000 powder diffract meter (Cu K α (λ = 1.5406 Å)) was exploited to obtain X-ray diffraction (XRD) pattern and a Jobin-Yvon LabRAM HR800 Raman Spectrometer to obtain Raman spectrum. The functional groups of 3D KIPIG were evaluated by Fourier transform infrared (FTIR) spectra (a PerkinElmer Spectrum One with KBr pellets method) and Xray photoelectron spectroscopy (XPS, a Kratos Ultra AXIS DLD XPS with a monochromated Al source). Inductively coupled plasma (ICP) was exploited to determine K+ concentration in 3D KIPIG. Element analysis (Model 240XA, Control Equipment Corporation) was carried out via the combustion approach to obtain oxygen content.

The 3D KIPIG electrode was fabricated by mixing 3D KIPIG powder, carbon black, and poly(tetrafluoroethylene) with a weight ratio of 8:1:1 in isopropyl alcohol to form a homogeneous slurry. Then, the slurry was rolled to a rectangular strip and pressed on a 1 cm \times 1 cm nickel foam as current collector. Before the electrochemical test, the obtained electrode should be dried in an 80 °C oven for 24 h to remove the organic solvent of binder and isopropyl alcohol.

The aqueous symmetrical supercapacitor cell (as illustrated in Figure S1) was assembled with two identical 3D KIPIG electrodes as anode and cathode, a glassy microfiber filter (Whatman, GF/F) as separator, and 2 M KOH aqueous solution as electrolyte. An electrochemical workstation (Princeton Potentiostat/Galvvanostat Model 273A) was utilized to test the electrochemical performance of 3D KIPIG electrodes. Cyclic voltammetry (CV) at scan rate of 30–300 mV/s and galvanostatic charge/discharge cycling at current density of 1–10 A/g were carried out in potential range of 0–1 V. The test for wide operating temperature range was carried out in a water bath (55 °C) and ice bath (–15 °C). Besides, the electrolyte for the –15 °C test is a mixture of 70 wt % 2 M KOH aqueous solution and 30 wt % ethylene glycol.

ASSOCIATED CONTENT

S Supporting Information

The Supporting Information is available free of charge on the ACS Publications website at DOI: 10.1021/acs.iecr.7b05413.

Figures of symmetrical supercapacitor structure, XPS spectrum, and TEM and SEM images of materials (PDF)

AUTHOR INFORMATION

Corresponding Author

*Yun Hang Hu. E-mail: yunhangh@mtu.edu.

ORCID ®

Dario J. Stacchiola: 0000-0001-5494-3205 Yun Hang Hu: 0000-0002-5358-8667

Author Contributions

Y.H.H. supervised the project and designed the material synthesis approach. L.C. synthesized materials, fabricated devices, tested device performances, and conducted material characterizations except XPS. D.S.S. performed XPS characterization. All authors were involved in analysis and discussion of results. Y.H.H. and L.C. wrote the manuscript with input from all other authors.

Notes

The authors declare no competing financial interest.

■ ACKNOWLEDGMENTS

This contribution was identified as the Best Presentation in the session "Carbon Management: Advances in Carbon Efficiency, Capture, Conversion, Utilization & Storage" of the 2017 ACS Fall National Meeting in Washington, DC. This work was supported by U.S. National Science Foundation (CMMI-1661699). L.C and Y.H.H. also thank Charles and Carroll McArthur for their great support.

REFERENCES

(1) Larcher, D.; Tarascon, J. M. Towards greener and more sustainable batteries for electrical energy storage. *Nat. Chem.* **2015**, *7*, 19–29.

- (2) Mai, L.; Tian, X.; Xu, X.; Chang, L.; Xu, L. Nanowire electrodes for electrochemical energy storage devices. *Chem. Rev.* **2014**, *114*, 11828–11862.
- (3) Bonaccorso, F.; Colombo, L.; Yu, G.; Stoller, M.; Tozzini, V.; Ferrari, A. C.; Ruoff, R. S.; Pellegrini, V. Graphene, related two-dimensional crystals, and hybrid systems for energy conversion and storage. *Science* **2015**, 347, 1246501.
- (4) Yu, G.; Xie, X.; Pan, L.; Bao, Z.; Cui, Y. Hybrid nanostructured materials for high-performance electrochemical capacitors. *Nano Energy* **2013**, *2*, 213–234.
- (5) Simon, P.; Gogotsi, Y.; Dunn, B. Where do batteries end and supercapacitors begin? *Science* **2014**, *343*, 1210–1211.
- (6) Wang, G.; Zhang, L.; Zhang, J. A review of electrode materials for electrochemical supercapacitors. *Chem. Soc. Rev.* **2012**, *41*, 797–828.
- (7) Zhang, S.; Pan, N. Supercapacitors performance evaluation. *Adv. Energy Mater.* **2015**, *5*, 1401401.
- (8) Vellacheri, R.; Al-Haddad, A.; Zhao, H.; Wang, W.; Wang, C.; Lei, Y. High performance supercapacitor for efficient energy storage under extreme environmental temperatures. *Nano Energy* **2014**, *8*, 231–237.
- (9) Chang, L.; Wei, W.; Sun, K.; Hu, Y. H. 3D flower-structured graphene from CO₂ for supercapacitors with ultrahigh areal capacitance at high current density. *J. Mater. Chem. A* **2015**, 3, 10183–10187.
- (10) Sun, H.; Mei, L.; Liang, J.; Zhao, Z.; Lee, C.; Fei, H.; Ding, M.; Lau, J.; Li, M.; Wang, C.; Xu, X.; Hao, G.; Papandrea, B.; Shakir, I.; Dunn, B.; Huang, Y.; Duan, X. Three-dimensional holey-graphene/niobia composite architectures for ultrahigh-rate energy storage. *Science* 2017, 356, 599–604.
- (11) Zhu, Y.; Murali, S.; Stoller, M. D.; Ganesh, K. J.; Cai, W.; Ferreira, P. J.; Pirkle, A.; Wallace, R. M.; Cychosz, K. A.; Thommes, M.; Su, D.; Stach, E. A.; Ruoff, R. S. Carbon-based supercapacitors produced by activation of graphene. *Science* **2011**, *332*, 1537–1541.
- (12) Xu, Y.; Chang, L.; Hu, Y. H. KOH-assisted microwave post-treatment of activated carbon for efficient symmetrical double-layer capacitors. *Int. J. Energy Res.* **2017**, 41, 728–735.
- (13) Yu, D.; Goh, K.; Wang, H.; Wei, L.; Jiang, W.; Zhang, Q.; Dai, L.; Chen, Y. Scalable synthesis of hierarchically structured carbon-nanotube-graphene fibres for capacitive energy storage. *Nat. Nanotechnol.* **2014**, *9*, 555–562.
- (14) Chang, L.; Stacchiola, D. J.; Hu, Y. H. An ideal electrode material, 3D surface-microporous graphene for supercapacitors with ultrahigh areal capacitance. ACS Appl. Mater. Interfaces 2017, 9, 24655–24661.
- (15) Chang, L.; Stacchiola, D. J.; Hu, Y. H. Direct conversion of $\rm CO_2$ to meso/macro-porous frameworks of surface-microporous graphene for efficient asymmetrical supercapacitors. *J. Mater. Chem. A* **2017**, *5*, 23252–23258.
- (16) Li, Y.; Zhao, Y.; Cheng, H.; Hu, Y.; Shi, G.; Dai, L.; Qu, L. Nitrogen-doped graphene quantum dots with oxygen-rich functional groups. *J. Am. Chem. Soc.* **2012**, *134*, 15–18.
- (17) Yang, X.; Cheng, C.; Wang, Y.; Qiu, L.; Li, D. Liquid-mediated dense integration of graphene materials for compact capacitive energy storage. *Science* **2013**, *341*, 534–537.
- (18) Mai, L.; Hu, B.; Chen, W.; Qi, Y.; Lao, C.; Yang, R.; Dai, Y.; Wang, Z. L. Lithiated MoO₃ nanobelts with greatly improved performance for lithium batteries. *Adv. Mater.* **2007**, *19*, 3712–3716.
- (19) Chang, L.; Hu, Y. H. Excellent capacitive deionization performance of meso-carbon microbeads. *RSC Adv.* **2016**, *6*, 47285–47291.
- (20) Bi, H.; Lin, T.; Xu, F.; Tang, Y.; Liu, Z.; Huang, F. New graphene form of nanoporous monolith for excellent energy storage. *Nano Lett.* **2016**, *16*, 349–352.
- (21) Qie, L.; Chen, W.; Xu, H.; Xiong, X.; Jiang, Y.; Zou, F.; Hu, X.; Xin, Y.; Zhang, Z.; Huang, Y. Synthesis of functionalized 3D hierarchical porous carbon for high-performance supercapacitors. *Energy Environ. Sci.* **2013**, *6*, 2497–2504.
- (22) Yu, Z.; Tetard, L.; Zhai, L.; Thomas, J. Supercapacitor electrode materials: nanostructures from 0 to 3 dimensions. *Energy Environ. Sci.* **2015**, *8*, 702–730.

- (23) Kim, N. D.; Buchholz, D. B.; Casillas, G.; Jose-Yacaman, M.; Chang, R. P. H. Hierarchical design for fabricating cost-effective high performance supercapacitors. *Adv. Funct. Mater.* **2014**, *24*, 4186–4194. (24) Tan, Y. B.; Lee, J. M. Graphene for supercapacitor applications. *J. Mater. Chem. A* **2013**, *1*, 14814–14843.
- (25) Roberts, A. J.; Slade, R. C. T. Performance loss of aqueous MnO₂/carbon supercapacitors at elevated temperature: cycling vs. storage. *J. Mater. Chem. A* **2013**, *1*, 14140–14146.
- (26) Chang, L.; Wei, W.; Sun, K.; Hu, Y. H. Excellent performance of highly conductive porous Na-embedded carbon nanowalls for electric double-layer capacitors with a wide operating temperature range. *J. Mater. Chem. A* **2017**, *5*, 9090–9096.
- (27) Choi, N. S.; Chen, Z.; Freunberger, S. A.; Ji, X.; Sun, Y. K.; Amine, K.; Yushin, G.; Nazar, L. F.; Cho, J.; Bruce, P. G. Challenges facing lithium batteries and electrical double-layer capacitors. *Angew. Chem., Int. Ed.* **2012**, *51*, 9994–10024.
- (28) Roberts, A. L.; Danil de Namor, A. F. R.; Slade, C. T. Low temperature water based electrolytes for MnO₂/carbon supercapacitors. *Phys. Chem. Chem. Phys.* **2013**, *15*, 3518–3526.